

Self-Assembly of Bioelastomeric Structures from Solutions: Mean-Field Critical Behavior and Flory–Huggins Free Energy of Interactions

F. SCIORTINO,^{1,*} K. U. PRASAD,² D. W. URRY,² and M. U. PALMA³

¹Graduate School of Physics, University of Palermo, Via Archirafi 36, I-90123 Palermo, Italy; ²Laboratory of Molecular Biophysics, The University of Alabama at Birmingham, P. O. Box 300, University Station, Birmingham, Alabama 35294; and ³Institute for Interdisciplinary Applications of Physics, National Research Council, and Department of Physics, University of Palermo, Via Archirafi, 36, I-90123 Palermo, Italy

SYNOPSIS

Elastic and quasi-elastic light scattering studies were performed on aqueous solutions of poly(Val-Pro-Gly-Gly), a representative synthetic bioelastomer that differs from the previously studied poly(Val-Pro-Gly-Val-Gly) by the deletion of the hydrophobic Val in position four. When the spinodal line was approached from the region of thermodynamic stability, the intensity of light scattered by fluctuations, and the related lifetime and correlation length, were observed to diverge with mean-field critical exponents for both systems. Fitting of the experimental data allowed determining the spinodal and binodal (coexistence) lines that characterize the phase diagrams of the two systems, and it also allowed a quantitative sorting out of the enthalpic and entropic contributions to the Flory–Huggins interaction parameters. The contribution of valine is derived by comparison of the two cases. This can be viewed as sorting out the effect of a modulation of the solute. The same approach may allow sorting out the entropic and enthalpic effect of modulations of the solvent by cosolutes (or by cosolvents). This could be of particular interest in the case of small osmolytes, affording important adaptive roles in nature, at the cost of very limited changes in genetic information.

Finally, the suggestion is further supported that statistical fluctuations of anomalous amplitude, such as those occurring in proximity of the spinodal line, have a role in promoting the process of self-assembly of extended supramolecular structures. On the practical side, the present approach appears useful in the design of novel synthetic model systems for bioelastomers. © 1993 John Wiley & Sons, Inc.

INTRODUCTION

Increasingly, attention is being focused on physical mechanisms underlying the self-assembly of extended structures from initially homogeneous systems. In the case of biologically significant structures, these studies are particularly interesting yet complex. From the point of view of physical studies, problems become more manageable whenever it is possible to work with well-known and characterized

systems of biomolecules (or representative synthetic model systems) having closely equal molecular mass and composition. Still, even in such cases, attempts to reach universal descriptions in terms of ordering transitions often meet serious difficulties due to sensitivity of self-assembly processes to molecular detail and to small changes in key parameters.^{1–3} For this reason, to identify some common and general process governing the self-assembly of biologically significant order in widely different systems appears particularly appealing.⁴

Elastic and quasi-elastic light scattering studies of solutions of significant biopolymers have recently shown that the clustering of polymers due to spontaneous fluctuations of concentration, undamped as

well as damped, may have an important role in promoting significant biomolecular encounters leading to the self-assembly of extended structures. In the case of undamped fluctuations (leading to spinodal decomposition) the order parameter, correlation length, and connectivity features of a biologically significant self-assembled supramolecular structure have been found to reflect those of the decomposed sol.^{5,6} The (spinodally) decomposed sol appears thus capable of providing a canvas for the self-assembly of supramolecular structures.^{7,8} Damped, anomalously large (and progressively slower) fluctuations observed when a region of thermodynamic instability is approached also seem capable of initiating the local molecular and supramolecular order leading to the self-assembly of extended structures.^{4,9,10} In previous studies high molecular weight poly(Val-Pro-Gly-Val-Gly), abbreviated poly(VPGVG) or simply PPP, has been used.⁹⁻¹¹ This is a particularly attractive model for the natural elastomeric protein, as it is the most striking primary structural feature of bovine¹² and porcine¹³ elastins, and as it exhibits many properties, including elasticity, which are remarkably similar to those of the natural protein.¹⁴⁻¹⁶ The possibility of preparing synthetic poly(VPGVG) with molecular weight in excess of 50 kD,¹⁴ and knowledge of the primary and secondary structure,¹⁷ of emerging hydrophobic tertiary and quaternary contacts,^{18,19} of its remarkable dynamic properties,^{15,20} which are the basis for its most important elastic properties, and of its demonstrated self-assembly into fibers,¹⁴ makes poly(VPGVG) particularly well suited for *in vitro* studies of self-assembly processes in biomolecular systems. Notably, its aggregation process becomes representative of many biological assembly processes where hydrophobic interactions have a dominant role. With the particular care necessary to assure no significant racemization in the chemically synthesized product, it has been possible to develop a hydrophobicity scale of all of the naturally occurring amino acids in different ionization states where relevant, and with biologically relevant chemical modifications based on the temperature for the onset of the hydrophobic folding and assembly process.^{21,22} The general formula of the polypentapeptides is poly[f_v VPGVG, f_x (VPGXG)] where f_v and f_x are mole fractions with $f_v + f_x = 1$, and x is any of the naturally occurring amino acid residues or modifications thereof.

A related polytetrapeptide, poly(VPGG) or PTP, which has also been identified in natural elastin^{23,24} and which obviously differs from poly(VPGVG) by the deletion of the valine residue in position four, is also substantially characterized as to conforma-

tion,²⁵ and as to its filamentous²⁶ and elastic²⁷ nature. For this reason its study promised to shed light, by comparison with PPP, on the contribution of the valyl hydrophobic residue to the thermodynamics of this system. In the forthcoming sections we report the phase diagram of PTP including both the spinodal and coacervation lines as obtained by a combined use of elastic light scattering and photon correlation spectrometry.^{9,10} Further, the present results are analyzed (and compared with previous results relative to PPP) in terms of the mean-field Flory-Huggins expression for the free energy.²⁸ The enthalpic and entropic contributions to the interaction parameter are obtained in the two cases by a fitting procedure. For both PPP and PTP the analysis is here extended to obtain not only the spinodal but also the coexistence line. Using a mean-field approach in studying the transition to self-assembled bioelastomeric structures of PPP and PTP is consistent with the fact that in both cases the correlation length of concentration fluctuations and the intensity of light scattered by them were measured to diverge with mean-field exponents on approaching the spinodal line from the region of stability. The correctness of our approach will be better discussed in the following. The functional potentiality of damped concentration fluctuations⁴ will also be discussed.

MATERIALS AND METHODS

Sample Preparation

The synthesis of the poly(Val-Pro-Gly-Gly) was carried out as previously described.²⁷ The mean molecular weight is approximately 100 kD, corresponding to a degree of polymerization of about 300 tetramer units. Polytetrapeptide was mixed with an excess of deionized, distilled water (Millipore SQ) and dissolved at temperatures below 20°C. The solution was subsequently filtered through a 0.22- μ Millipore filter directly in the cuvette used for the experiments, and then placed in a thermostated bath at 80°C. Upon standing overnight at this temperature, a well-defined coacervate phase was obtained, and the overlying equilibrium solution was removed. The coacervate phase concentration, determined a posteriori as 189 mg of polymer in 0.41 mL solution (460 mg/mL), was the highest concentration used in the present study. Fifteen different (lower) concentrations were obtained by successive dilutions of the same sample with known quantities of Millipore SQ water. An aliquot of the solution so obtained at

about the eighth dilution was lyophilized and its concentration measured. The concentration values for samples obtained by previous and following dilutions was determined in this way to an overall precision of 10%, most variation of which was due to a systematic error. Concentration values have been changed from milligram per milliliter to volume fraction units assuming a constant polymer density of 1 gm/mL. This assumption will be discussed below.

Experimental

Each sample was subjected to a slow, upward temperature scan (0.03°C/min) from about 20°C to the coacervation (cloud point) temperature. The intensity of light scattered at 90°, the autocorrelation function of the quasi-elastically scattered light (QELS), and the intensity of the beam transmitted through the sample were simultaneously recorded throughout the temperature scan as previously described.¹¹ The absence of any difference between data recorded at any given temperature during the slow scan and those obtained in isothermal conditions has been accurately checked. The experimental setup and methodology used to analyze data were also previously described.^{5,11}

RESULTS

Figure 1 contains the complete phase diagram of the PTP-water solution in the T, c plane and includes both the cloud point line and the spinodal line. The cloud point line was determined by measuring for each concentration the temperature T_{cl} , at which the intensity of the transmitted beam essentially vanishes, as a consequence of the large multiple scattering accompanying the onset of coacervation.²⁸ To determine the spinodal line, we have used the scattering method,²⁹⁻³¹ modified so as to use QELS data for subtracting spurious contributions.⁹ The scattering method makes use of the relation of inverse proportionality existing, in the hydrodynamic regime, between the intensity of the light scattered by a homogeneous binary solution and the second derivative of the Gibbs free energy of the solution itself.²⁹ The spinodal temperature T_{SP} is determined by extrapolating to zero the straight-line fitting of the reciprocal of the scattered intensity vs temperature, in the region of stability. To obtain the spinodal line, the procedure is repeated at several concentration values. The quality of data was similar to that previously obtained.^{9,11} Actual profiles of the

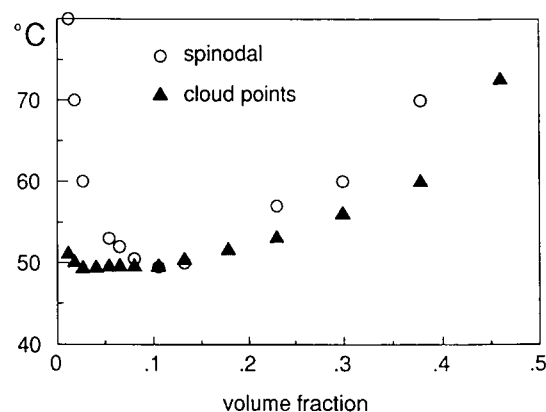


Figure 1. Complete phase diagram of the poly(Val-Pro-Gly-Gly)-water system. Full triangles: cloud points; circles: spinodal. Precision of the experimental data is within 0.2°C for cloud point values (T_{cl}) and from 0.4 to 4°C for spinodal point values (T_{SP}). The uncertainty increases progressively with the distance between spinodal and cloud point curves, due to the extrapolation procedure used to determine T_{SP} (see Ref. 8).

reciprocal of the scattered intensity of light vs temperature are presented in this section, along with similar profiles for the correlation length of fluctuations. As shown in Figure 1, the spinodal and the cloud points superpose at about $\Phi = 10\%$ and $T = 50^\circ\text{C}$. This is thus the critical point for the system. Note that this point is slightly shifted to the right of the threshold cloud point, as theoretically expected for solutions of polymers having some degree of polydispersity.³²

QELS experiments were used for measuring the decay time of concentration fluctuations.^{9,10} Data on the raw decay times of the photon correlation function, after subtraction of the spurious contribution as previously described,¹¹ are shown in Figure 2a. Now we observe from Figure 1 that at constant temperature in the region of stability, the distance from the spinodal line decreases at increasing concentration up to the critical value $\Phi = 10\%$. Correspondingly, Figure 2a demonstrates an increase in the fluctuation decay time with concentration up to this critical value. This behavior agrees with theoretical expectations and, as it is easily seen, with the measured increase of scattered light intensity.²⁸ Actually, in terms of the mode-mode coupling model³² and for conditions wherein the mean size ξ of fluctuations is smaller than the reciprocal of the scattering vector, it is

$$\xi = \frac{kTQ^2\tau}{6\pi\eta} \quad (1)$$

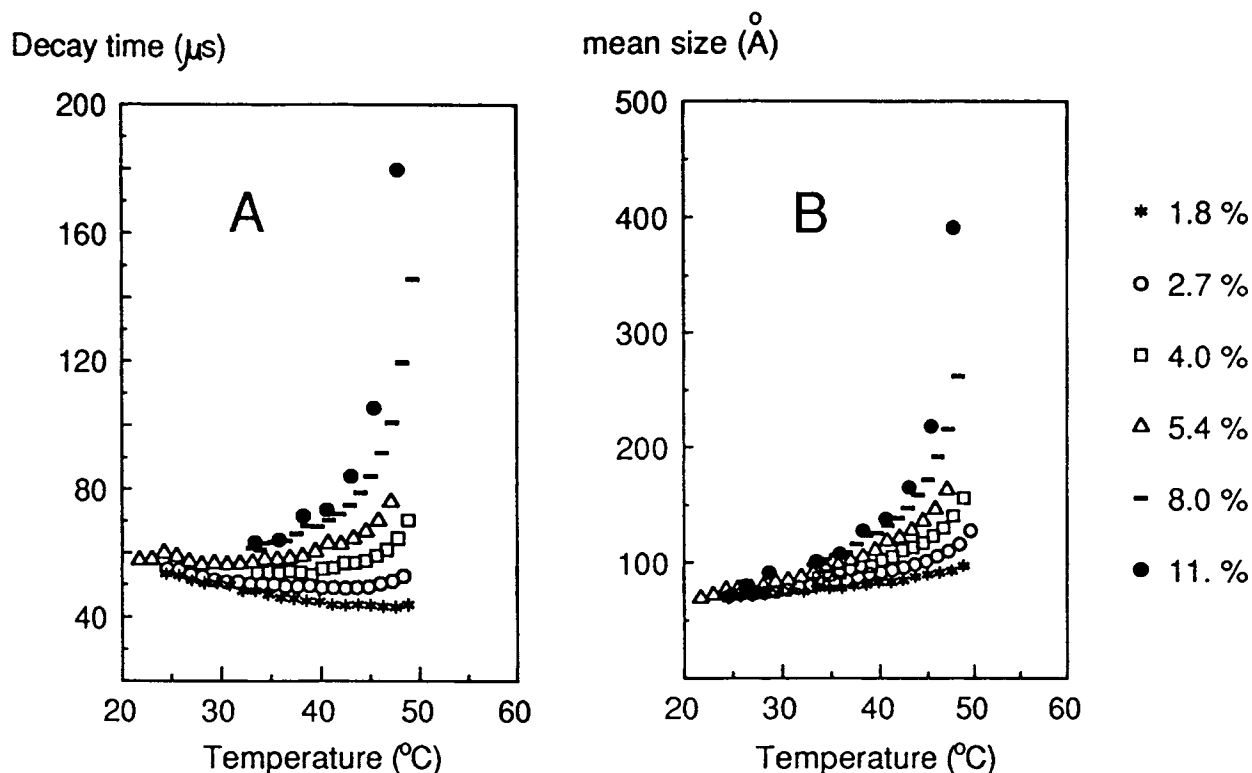


Figure 2. (a) Decay times of polymer concentration fluctuations as a function of temperature in the single phase region. (b) Mean size of fluctuations in polymer concentration. Note that at low temperatures this value is concentration independent and coincides with the measured hydrodynamic radius of polymer coils.

where τ is the measured decay time of the nonspurious component^{9,11} of the autocorrelation function, η is the viscosity, Q is the scattering wave vector, and k is the Boltzmann constant. For our conditions the reciprocal of the scattering vector is about 50 nm, ten times larger than the maximum ξ value derived from Eq. (1), so that it is safe to assume that the latter describes appropriately the behavior of the mean size of concentration fluctuations and, in particular, its diverging behavior as τ diverges. Values of ξ obtained using Eq. (1) are actually shown in Figure 2b. Now, noting that Eq. (1) coincides with the equation describing the diffusion coefficient of a sphere of radius ξ in a liquid, the lowest ξ in Figure 2b that appears to be essentially independent of temperature in the lower range of temperatures, and also independent of concentration at the lowest temperatures, corresponds with the average hydrodynamic radius of the random coil polymers. Actual numerical values shown in Figure 2a were derived using the known viscosity values of the solvent in Eq. (1). While using the viscosity of the solvent rather than that of the solution might appear objectionable, it must be remarked that neither of the

two choices is strictly satisfactory.^{33,34} Nevertheless, using the solvent viscosity values makes the low-temperature data consistent with the hydrodynamic radii of polymer coils over a very wide range of concentrations (see Figure 2b). Also, as can be seen by comparing (a) and (b) of Figure 2, this choice does not alter the general behavior already shown by the raw QELS data. Finally, it is clear that the increase with temperature of the "mean size" in Figure 2b cannot be due to a trivial swelling of the polymer coil, because of its dependence upon concentration and of the fact that at higher temperatures hydrophobic forces will tend to compress the polymer coils.

In Figure 3 for PTP is plotted the temperature dependence of the reciprocal of scattered light intensity I^{-1} and ξ^{-2} (the reciprocal square of values given in Figure 2b) for two concentrations. The nearly linear dependence of both I^{-1} and ξ^{-2} on temperature demonstrates that the intensity of scattered light, and the correlation length of concentration fluctuations that are responsible for the scattering, diverge with the mean-field critical exponent 1 and 0.5, respectively. In the mean-field approximation, as it is known, the state of any selected

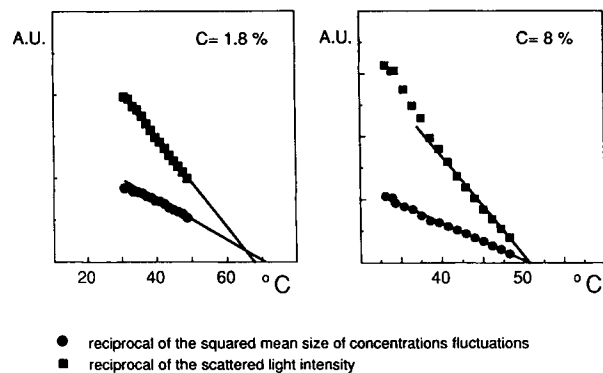


Figure 3. Reciprocal of scattered light intensity and reciprocal of the squared mean size of concentration fluctuations for two selected concentrations of poly(Val-Pro-Gly-Gly). Note the close fit in terms of mean-field critical exponents and the coincidence (within the stated accuracy) of T_{SP} . Also note that only one of the two concentrations is close to the critical point.

particle of the system is assumed to be determined by the average properties of the system as a whole. The assumption is not granted for disperse or paucidisperse polymeric solutions, and as we shall see in the next section, it is of theoretical and practical interest that it applies to the present case.

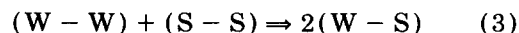
DISCUSSION

It is useful to analyze the experimentally determined phase diagram of PPP-water¹¹ and PTP-water solutions in terms of the mean-field (Flory-Huggins) treatment³⁵ of the stability of solutions of flexible polymers.²⁸ Appropriateness of this treatment to the present case is suggested by the observed mean-field divergences of the mean size and of the decay time of concentration fluctuations (Figures 2 and 3), but we shall subject it to closer scrutiny. In the classic Flory-Huggins approach, the random-coiled polymer chains are taken as random walks on a lattice, each lattice site being either occupied by one chain segment or by solvent. The mesoscopic (coarse-grained) free energy of mixing F for a solution of paucidisperse polymers can then be written as¹

$$\left. \frac{F}{T} \right|_{\text{site}} = \frac{\Phi_P}{N_P} \ln \Phi_P + \Phi_W \ln \Phi_W + \chi \Phi_P \Phi_W \quad (2)$$

where the temperature is in energy units, N_P is the number of orientationally independent segments in the polymer chain, Φ_P and Φ_W (where $\Phi_P + \Phi_W = 1$) indicate the volume fraction of polymer p and

solvent w , respectively. The Flory interaction parameter χ is a nondimensional quantity measuring the enthalpy change per site (or $\Delta H/T$ in the present notation) accompanying the creation of nearest neighbor solvent (W) and segment (S) pairs from nearest neighbor $W-W$ and $S-S$ pairs. This process is schematically represented as



It appears clear from Eq. (2) that polymers having large N_P values exhibit a very small entropy of mixing. Thus, subtle differential effects, difficult to observe in small-molecule systems, are amplified in polymers. As may be better appreciated from what follows, this adds to the adaptability of biopolymers to altered function at small cost in terms of genetic modifications.

For aqueous solutions of biopolymers, the formation of a $S-W$ pair alters the solvent structure and dynamics,³⁶⁻³⁸ as well as the polymer conformation and dynamics. In fact, several biomolecular processes are characterized by entropy variations with hydrophobic and vibrational contributions of comparable sizes.³⁹ These effects can be taken into account by adding an entropy term to χ so that^{11,28}

$$\chi = \frac{\Delta H}{T} - \Delta S \quad (4)$$

where $\Delta H - T\Delta S$ measures the free energy change per site ΔF associated with the process of Eq. (3) and ΔS is in K_B units. The curvature of $F(\Phi)$ determines the stability properties of the polymer solution and the associated phase diagram in the (Φ, χ) plane. In particular, the instability region is encompassed by the spinodal line, defined by

$$\frac{\partial^2}{\partial \Phi_P^2} \left(\frac{F}{T} \right) = 0 \quad (5)$$

that is,

$$\frac{1}{N_P \Phi_P} + \frac{1}{(1 - \Phi_P)} - 2\chi = 0 \quad (6)$$

This expression [with χ defined as in Eq. (4)] can be conveniently used for fitting the experimental points $T_{SP}(\Phi)$ for both PPP and PTP. In this way best-fit values of ΔH , ΔS , and N_P are obtained as shown in Table I. In this approximation the interaction enthalpy and entropy terms of ΔH and ΔS are assumed to be independent of temperature and

Table I Values of Parameters Used in Eq. (4) to Generate the Full Lines Reported in Figure 3^a

	ΔH Site (kJ/mol)	ΔS Site (J/K mol)	$\Delta H/\Delta S$ (K)	N_P
PPP				
Spinod	-15.7	-57	275	51
Coex	-15.7	-57.5	273	
PTP				
Spinod	-10.2	-37	276	97
Coex	-10.2	-36.6	279	

^a ΔH and ΔS measure the enthalpy and entropy variation associated with the process of Eq. (3). N_P is the average number of independent segments comprising the polymer. Spinod and coex indicate the values used to obtain the spinodal and coexistence lines, respectively, in Figure 4. As seen, these different sets of values lie remarkably close.

sample concentration (within the small spans required by our experiments).

The coexistence line is the locus of point pairs having at each temperature equal chemical potentials, as given by the two simultaneous equations:

$$\begin{aligned} \ln(1 - \phi'_P) + (1 - N_P^{-1})\phi'_P + \chi(\phi'_P)^2 \\ = \ln(1 - \phi''_P) + (1 - N_P^{-1})\phi''_P + \chi(\phi''_P)^2 \\ \ln \phi'_P - (N_P - 1)(1 - \phi'_P) + N_P\chi(1 - \phi'_P)^2 \\ = \ln \phi''_P - (N_P - 1)(1 - \phi''_P) \\ + N_P\chi(1 - \phi''_P)^2 \quad (7) \end{aligned}$$

For each chosen temperature, the two corresponding points of the coexistence line were obtained by solving Eq. (7) numerically. To this purpose, parameter values obtained from the spinodal data and shown in Table I were used. Coexistence lines obtained by this procedure for both PTP and PPP are given in Figure 4, which also shows the corresponding spinodal lines obtained by the already discussed best fittings of the experimental (extrapolated) T_{SP} points. In this way the full phase diagrams for PTP and PPP having the specific molecular mass used in the present work are obtained, along with the method for deriving such phase diagrams in other similar cases. Note that as a consequence of the fast coacervation kinetics, the experimentally determined glow points are expected to lie not far from the lower boundary of the metastable (nucleated) region, which is the coexistence line.

The N_P values given in Table I measure the "effective number of independent segments" in individual polymers, making an "effective flexible chain." For both polypeptides N_P is seen to be

smaller than the approximate total number of residues in the polymers chains. This implies a certain degree of stiffness of the polymer chain (that is, some orientational correlation at least among some individual residues). Notwithstanding the internal consistency of the experimental data, and of spinodal and coexistence lines fitting them, this stiffness might be suspected to invalidate application in the present case of the classic Flory-Huggins treatment, originally developed for flexible polymers. Further developments of the same theory, appropriate to more complex cases of semiflexible polymers,⁴⁰⁻⁴² could be thought to offer a better interpretation of the data, and thus quantitatively more reliable ΔH and ΔS values. As we are going to see below, however, this is not the case, and our polymers can in fact be considered (at temperatures below coacervation) as flexible random coils of "effective units," each unit consisting of more than one orientationally correlated residues.

It must be remarked that the semiflexible polymer chains shown by Flory to behave in such a distinctly different manner compared to the flexible case are those characterized by a tendency of their individual segments "to arrange themselves in co-linear succession."⁴² Now, while colinear stiffness results in rod-like (or elongated) shapes, stiffness per se does not need to cause elongated shapes and can in fact give origin even to globular ones. In our specific

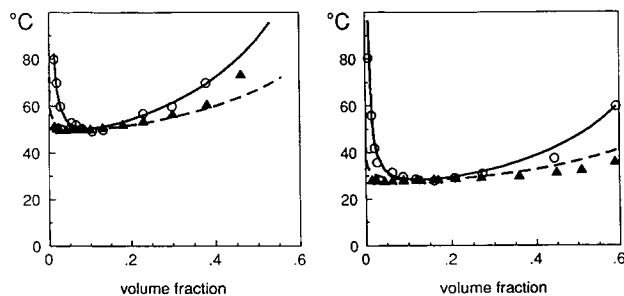


Figure 4. Complete phase diagram, including spinodal (solid) and coexistence (broken) lines for poly(Val-Pro-Gly-Val-Gly)-water (right) and poly(Val-Pro-Gly-Gly)-water (left) solutions. Full lines have been generated using the values reported in Table I in the Flory-Huggins mean-field analytical expression [Eqs. (6) and (7), respectively]. Experimental spinodal points (circles) were obtained by the extrapolation procedure described in the text. Experimental points lying on (or close to) the coexistence lines were determined as glow points (full triangles). Glowing of laser-irradiated specimen, due to multiple light scattering, monitors the onset of coacervation and it occurs within a temperature interval narrower than the size of symbols used in the figure.

case, ample evidence points out that partial stiffness of the random coils can be attributed to β -turns^{14,19,43,44} and the latter do not certainly favor colinear successions. Further, our data show no evidence whatsoever of the occurrence in the phase diagrams of Figure 4 of the distinct spike-like feature (immiscibility gap) predicted by Flory for the case of semiflexible polymers.⁴⁰⁻⁴²

Unsuitability of the treatment relative to colinearly semistiff polymers does not legitimate, however, using the treatment appropriate to the case of perfect flexibility, and we must look deeper into it. Let us evaluate the average size ξ_a of those polymer segments that are to a large extent independently orientable. To this purpose we use the random walk relation that links the mean end-to-end R polymer distance to the number of independent units in an ideal chain^{1,35}

$$R = \xi_a N_P^\nu \quad (8)$$

where ν is 0.5 in the ideal case and 0.6 when the need of a self-avoiding random walk is taken into account. Using the N_P values reported in Table I and taking for R the hydrodynamic radii (50 Å for PPP and 70 Å for PTP) measured by QELS, the ξ_a values for either polymer are 7 and 4.6 Å for the ideal and self-avoiding case, respectively. It should be noted, however, that compression of the polymer coil due to hydrophobic interactions will have a compensating effect on the explosion due to self-avoidance, and make the 0.5 value for ν perhaps more realistic. In any case, ξ_a values given above compare well with the linear dimension of the β -turn structure,⁴³⁻⁴⁵ the elementary structural building block of the ordered β -spiral tertiary structure that is stable at high temperature.^{15,17} In short, this suggests that the pretransition random coil conformation of both PPP and PTP is that of a random coil of effective (orientationally free) polymer segments, each of which contains more than one residue. These residues are seen as orientationally correlated, not in a rod-like fashion but by way of more efficiently space-filling β -turns and suspended segments.^{14,19,43,44} This agrees very well with Raman⁴³ and nuclear Overhauser effect measurements,^{18,19} and with early nmr data,^{25,46,47} showing the presence of a typical β -turn structure also in the coil configuration at temperatures below the onset of aggregation. In this view we have only to do some scaling for what concerns the solvent, and consider an effective solvent molecule whose size is equal to the average size of an effective orientationally free polymer segment. This approach, which does not affect

the relationships used here,^{35,42} has actually been used with success in different contexts (see, e.g., Refs. 48-50).

Facts appear, then, to concur in pointing out that appropriate scaling allows describing the present case in terms of the classic Flory-Huggins theory. This conclusion is strengthened if we recall the closely mean-field divergences observed for both the size and lifetime of concentration fluctuation, independently measured by different experimental approaches (Figures 2 and 3). Further support comes from the internal consistency of N_P values in Table I, and from comparison of the theoretical and coexistence lines with experimental data in Figure 4.

We can now assign the ΔH and ΔS terms of Table I to the variation in enthalpy and entropy associated with the exposure of a polymer effective segment of length ξ_a to the solvent. The ΔS term is greater in PPP than in PTP, in agreement with the higher mean hydrophobicity of the polymer chain. The signs of ΔH and ΔS reported in Table I confirm the inverse-temperature nature of the phase separation process. With respect to the reported $\Delta H/\Delta S$ ratio, we note that numerous processes involving formation/breaking of hydrophobic interactions are characterized by a correlated variation in ΔH and ΔS , corresponding to a compensation temperature not far from 275 K.^{51,52}

As to the meaningfulness of numerical values in Table I, we note that fittings of the spinodal data remain acceptable, if not excellent, within 10-15% of the given (best-fit) parameters, and that the theoretical coexistence line derived from those best-fit parameter values lies close to the experimental glow points. In consideration of the observed internal consistency of our analysis, we think it reasonable to take all values given in Table I as meaningful within 10%. In particular, the difference *ceteris paribus* between PPP and PTP can be taken with confidence.

CONCLUDING REMARKS

In this work we have addressed the problem of viewing a specific process of self-assembly of a biologically relevant supramolecular order within the general framework of polymer science, thermodynamic stability, and phase transitions.⁵⁻¹¹ The experimental study was carried out on quasi-binary solutions of poly(Val-Pro-Gly-Gly), one of two representative synthetic polypeptide elastomers. This polytetrapeptide, or PTP, was the first identified repeating

sequence²¹ of the native bioelastomer, elastin, and it differs from the later found and most striking repeating peptide sequence, Poly(VPGVG), or PPP, by deletion of the hydrophobic valine residue in position four. The complete phase diagrams in the temperature-concentration plane are now established with reasonable accuracy for these two representative synthetic model systems of the native bioelastomer, elastin. The phase diagrams shown in the present paper refer to the specific polymer mass used. However, the ΔH and ΔS parameters, and the appropriateness of the approach used for obtaining the phase diagrams relative to higher mass similar polymers, remain established. In particular, and by comparison of the two cases of PPP and PTP, a quantitative evaluation of the contribution due to the hydrophobic valine residue is obtained. This is similar to the case of a quantitative evaluation of the thermodynamic effects of the pathological mutation of human hemoglobin HbA into HbS responsible for sickle cell anaemia.^{48,49} The average number of peptides linked as almost rigid yet noncolinear segments in the polymers, is in agreement with previous data obtained from totally different types of experiments.^{17-19,43-45}

Of particular interest is the possibility of evaluating quantitatively the enthalpic and the entropic contributions of single peptides to the generalized force that governs the stability of homogeneous solutions of these polymers, and that therefore drives toward the self-assembly of these extended structures. In fact, this offers new, direct views to the study of generalized solvent-induced forces^{48,49,53-55} as well as to the design of novel synthetic elastomers, to serve either as model systems of theoretical interest, or as new materials covering important practical applications.⁵⁶⁻⁵⁸ Also, it is useful in understanding chemomechanical transduction and other free energy transductional properties,^{21,59,60} and in quantifying the contribution of librational free energy to bioelastomeric restoring forces.

Data such as in Table I suggest two additional quantitative approaches to the design of new materials: by preferential linking of cosolutes capable of altering the average length of rigid segments in the polymer (thus affecting the N_p value in Table I), and by solvent modulation capable of affecting other parameters in Table I. The evolutionary potential, in terms of the economy of genetic information changes by way of solvent modulation by small osmolytes, has already been brought into focus.^{61,62} Thermodynamic data derived from the present approach will probably help in understanding the quantitative entropy-enthalpy interplay in

the case of such genetically important modulations of solute-solvent interactions and of solvent-mediated solute-solute interactions. Also, the reader may find it instructive to compare values in Table I to similar Flory-Huggins data concerning human deoxyhemoglobin A and S,^{48,49} and to differential scanning calorimetry (DSC) data on the polypeptide and its analogues.⁶³⁻⁶⁵ In so doing, it should be remembered that our ΔH and ΔS terms refer to an effective polymer segment that is longer than a single peptide, as a consequence of the discussed spatial correlations among adjacent amino acids. It is also necessary to recall that DSC data refer to the actual coacervation process, while Flory-Huggins parameters refer to the instability of the *solution as such*. That is, DSC data include the entropy of mixing as well as the enthalpic and entropic terms relative to the very process of coacervation, which includes the formation of β -spirals and assemblies of supercoiled β -spirals.^{15,19,43,44}

A more general remark concerns the divergences of amplitude and lifetime of the anomalous concentration fluctuations observed on approaching the spinodal line from the region of thermodynamic stability. In order to appreciate their possible effects, it is useful to distinguish between demixing and coacervation. Permanent demixing can occur via the spinodal or the nucleated process (depending on whether it starts from the instability or the metastability region), but it always is a liquid-liquid transition, governed by the Flory-Huggins free energy. However, divergences such as those in Figure 2 and 3 can be coarsely regarded as a transient demixing of longer and longer lifetime and larger amplitude. Coacervation, instead, is a process involving not only the mere clustering of polymers in specific regions of the specimen, but also polymer conformational changes and aggregation, with their own free energy terms. As a consequence of these changes, the coacervate polymers may become insoluble, and (more slowly) precipitate as in fact is observed in the present case. Coacervation causes the specimen to glow under the laser light, as a consequence of strong light scattering. Of course, demixing also per se may cause some glow, (although far less intense) because of its inherent inhomogeneities of concentration. As is clear from the text, glow points in Figures 1 and 4 indicate the onset of coacervation during the upward temperature scanning. In our case, the observed coacervation kinetics is very fast, and the numerical size n_{coac} of polymer aggregates necessary for local nucleation of coacervation is expected to be small. In such conditions, as soon as the concentration of solute polymers (lo-

cally enhanced either by actual demixing or by fluctuations having sufficiently long lifetime) will allow the local aggregation of a number n_{coac} (or larger) of polymers, coacervation must and will occur. It follows that the experimental glow points in Figure 4 are expected to lie slightly above, below, or upon the coexistence line, depending upon how n_{coac} compares with the amplitudes of the nucleated and of the transient clustering of polymers.

A similar "priming" role of fluctuations is expected and found in gelation processes,^{1,4,7,8} with differences due to the topological nature of the gelation transition (see Ref. 1, pp. 150–152). More in general, a "transient demixing," as the one evidenced in Figures 2 and 3, can very effectively allow or favor concentration-dependent processes capable of occurring on a time scale shorter than that of fluctuation decay. The transient clustering due to concentration fluctuations of anomalous amplitude in the vicinity of the spinodal line is of course a property common to all polymeric solutions. However, their effectiveness in priming specific concentration-dependent processes depends primarily upon the availability and time scale of such processes in each specific case. Whenever such processes are available and occurring on a convenient time scale, anomalous concentration fluctuations may effectively favor them, even at low average concentrations where they would not occur in strictly homogeneous solutions.⁴

The input of several clarifying discussions with Professor M. B. Palma-Vittorelli, Dr. P. L. San Biagio, and Dr. D. Bulone is gratefully acknowledged. Also, we wish to thank Dr. M. A. Iqbal for the material used for the data in Figure 4, and Dr. D. Giacomazza, Mr. M. Lapis, and Mr. G. La Gattuta for help with the experiments. QELS experiments were done at IAIF-CNR. Support from CRRN-SM and MPI (60%) grants are also gratefully acknowledged, as is National Institute of Health Grant No. HL29578 to Dr. Dan W. Urry.

REFERENCES

- de Gennes, P. G. (1979) *Scaling Concepts in Polymer Physics*, Cornell University Press, Ithaca, NY.
- Heermann, D. W. (1984) *Z. Phys. B Condensed Matter* **55**, 309–315.
- Heermann, D. W. (1984) *Phys. Rev. Lett.* **55**, 1126–1128.
- Palma Vittorelli, M. B. (1989) *Intl. J. Quantum Chem.* **35**, 113–124.
- San Biagio, P. L., Madonia, F., Newman, J. & Palma, M. U. (1986) *Biopolymers* **25**, 2255–2269.
- Leone, M., Sciortino, F., Migliore, M., Fornili, S. L. & Palma-Vittorelli, M. B. (1987) *Biopolymers* **26**, 743–761.
- Bulone, D. & San Biagio, P. L. (1991) *Chem. Phys. Letts.* **179**, 339–343.
- Emanuele, A., Di Stefano, L., Giacomazza, D., Trapanese, M., Palma-Vittorelli, M. B. & Palma, M. U. (1991) *Biopolymers* **31**, 859–868.
- Sciortino, F., Prasad, K. U., Urry, D. W. & Palma, M. U. (1988) *Chem. Phys. Lett.* **153**, 557–559.
- Sciortino, F., Palma, M. U., Urry, D. W. & Prasad, K. U. (1988) *Biochem. Biophys. Res. Commun.* **157**, 1061–1066.
- Sciortino, F., Urry, D. W., Palma, M. U. & Prasad, K. U. (1990) *Biopolymers* **29**, 1401–1407.
- Yeh, H., Ornstein-Goldstein, N., Indik, Z., Sheppard, P., Anderson, N., Rosenbloom, J. C., Cicilia, G., Yoon, K. & Rosenbloom, J. (1987) *Collagen Related Res.* **7**, 235–247.
- Sandberg, L. B., Soskel, N. T. & Leslie, J. B. (1981) *N. Engl. J. Med.* **304**, 566–579.
- Urry, D. W. (1982) *Method Enzymol.* **82**, 673–716.
- Urry, D. W. (1988) *J. Protein Chem.* **7**, 1–34.
- Urry, D. W. & Prasad, K. U. (1985) in *Biocompatibility of Tissue Analogues*, Williams, D. F., Ed., CRC Press, Boca Raton, FL, pp. 89–116.
- Urry, D. W. (1984) *J. Protein Chem.* **3**, 403–436.
- Chang, D. K., Venkatachalam, C. M., Prasad, K. U. & Urry, D. W. (1989) *J. Biomol. Struct. Dynam.* **6**, 851–858.
- Urry, D. W., Chang, D. K., Krishna, R., Huang, D. H., Trapane, T. L. & Prasad, K. U. (1989) *Biopolymers* **28**, 819–833.
- Chang, D. K. & Urry, D. W. (1989) *J. Comput. Chem.* **10**, 850–855.
- Urry, D. W., (199262) *Prog. Biophys. Mol. Biol.* **57**, 23–57.
- Urry, D. W., Gowda, D. C., Parker, T. M., Luan, C. H., Reid, M. C., Harris, C. M., Pattanaik, A. & Harris, R. D. (1992) *Biopolymers* **32**, in press.
- Gray, W. R., Sandberg, L. B. & Foster, J. A. (1973) *Nature* **246**, 461–466.
- Sandberg, L. B., Leslie, J. G., Leach, C. T., Torres, V. L., Smith, A. R. & Smith, D. W. (1985) *Pathol. Biol.* **33**, 266–274.
- Khaled, M. A., Prasad, K. U., Vankatchalam, C. M. & Urry, D. W. (1985) *J. Am. Chem. Soc.* **107**, 7139–7145.
- Long, M. M., Rapaka, R. S., Volpin, D., Pasquali-Ronchetti, I. & Urry, D. W. (1980) *Arch. Biochem. Biophys.* **201**, 445–452.
- Urry, D. W., Harris, R. D. & Long, M. M. (1982) *J. Biomed. Mater. Res.* **16**, 11–16.
- Kurata, M. (1982) *Thermodynamics of Polymer Solutions*, Harwood Academic Publishers, Chur, NY.
- Scholte, Th. G. (1971) *J. Polym. Sci. A* **29**, 1553–1577.
- Tanaka, T., Nishio, I. & Sun, S. T. (1981) in *Scattering Techniques Applied to Supramolecular and Nonequi-*

- librium Systems*, Chen, S. H., Chu, B. & Nossal, P., Eds., Plenum Press, New York, pp. 703-724.
31. Thompson, J. A., Schurtenberger, P., Thurston, G. M. & Benedek, G. B. (1987) *Proc. Natl. Acad. Sci.* **84**, 7079-7083.
 32. Kawasaki, K. (1976) in *Phase Transition and Critical Phenomena*, Vol. 5A, Domb, C. & Green M. S., Eds., Academic, London.
 33. Cummins, H. Z. (1984) in *Photon Correlation and Light Beating Spectroscopy*, Cummins, H. Z. & Pike, E. R., Eds., Plenum Press, New York, pp. 285-330.
 34. Ishikimoto, C. & Tanaka, T. (1977) *Phys. Rev. Lett.* **8**, 474-477.
 35. Flory, P. J. (1953) *Principles of Polymer Chemistry*, Cornell University Press, Ithaca, NY.
 36. Kauzmann, W. (1959) *Adv. Protein Chem.* **14**, 1.
 37. Palma-Vittorelli, M. B. & Palma, M. U. (1987) *Adv. Biosci.* **65**, 281-289.
 38. Palma, M. U. (1989) *Int. J. Quantum Chem.* **35**, 125-139.
 39. Sturtevant, J. M. (1977) *Proc. Natl. Acad. Sci.* **74**, 2236-2240.
 40. Flory, P. J. (1977) *Ber. Bunsen-Gesell., Phys. Chem.* **81**, 885-891.
 41. Flory, P. J., Abe, A. & Frost, R. S. (1978) *Macromolecules* **11**, 1119-1144 (six articles).
 42. Flory, P. J. (1956) *Proc. Roy. Soc.* **234A**, 60-73.
 43. Thomas, G. J., Jr., Prescott, B. & Urry, D. W. (1987) *Biopolymers* **26**, 921-934.
 44. Urry, D. W., Trapane, T. L., Sugano, H. & Prasad, K. U. (1981) *J. Am. Chem. Soc.* **103**, 2080-2089.
 45. Cook, J. W., Einspahar, H. M., Trapane, T. L., Urry, D. W. & Bugg, C. E. (1980) *J. Am. Chem. Soc.* **102**, 5502-5505.
 46. Urry, D. W., Mitchell, L. W. & Ohnishi, T. (1974) *Proc. Natl. Acad. Sci. USA* **71**, 3265-3269.
 47. Urry, D. W., Mitchell, L. W. & Ohnishi, T. (1974) *Biochem. Biophys. Res. Commun.* **59**, 62-69.
 48. San Biagio, P. L. & Palma, M. U. (1991) *Biophys. J.* **60**, 508-512.
 49. San Biagio, P. L. & Palma, M. U. (1992) *Comm. Theor. Biol.*, in press.
 50. Miyazawa, S. & Jernigan, R. L. (1985) *Macromolecules* **18**, 534-552.
 51. Lumry, R. & Rajender, S. (1970) *Biopolymers* **9**, 1125-1227.
 52. Lauffer, M. A. (1985) *Entropy-Driven Processes in Biology*, Springer Verlag, Berlin, Heidelberg, and New York.
 53. Bulone, D., San Biagio, P. L., Palma-Vittorelli, M. B. & Palma, M. U. (1993) *J. Mol. Liquids*, in press.
 54. Bulone, D., Palma-Vittorelli, M. B. & Palma, M. U. (1992) *Intl. J. Quantum Chem.* **42**, 1427-1437.
 55. San Biagio, P. L., Bulone, D. & Palma, M. U. (1992) in *Proceedings of the International Workshop on Water-Biomolecule Interactions*, Conference Series of the Italian Physical Society, Palma, M. U., Parak, F. & Palma-Vittorelli, M. B., Eds., to appear.
 56. Urry, D. W., Parker, T. M., Nicol, A., Pattanaik, A., Minehan, D. S., Gowda, D. C., Morrow, C. & McPherson, D. T. (1992) *Am. Chem. Soc. Div. Polym. Mater. Sci. Eng.* **66**, 399-402.
 57. Urry, D. W. (1990) in *Cosmetic & Pharmaceutical Applications of Polym.*, Gebelein, C. G., Cheng, T. C. & Yang, V. C., Eds., Plenum Press, New York, pp. 181-192.
 58. Nicol, A., Gowda, D. C. & Urry, D. W. (1992) *J. Biomed. Mater. Res.* **26**, 393-413.
 59. Urry, D. W., Haynes, B., Zhang, H., Harris, R. D. & Prasad, K. U. (1988) *Proc. Natl. Acad. Sci.* **85**, 3407-3411.
 60. Urry, D. W. (1990) in *Protein Folding: Deciphering the Second Half of the Genetic Code*, Gierasch, L. M. & King, J., Eds., American Association for the Advancement of Science, pp. 63-71.
 61. Yancey, P. H., Clark, M. E., Hand, S. C., Bowlus, R. D. and Somero, G. N. (1982) *Science* **217**, 1214-1222.
 62. Arakawa, T. & Timasheff, S. N. (1985) *Biophys. J.* **47**, 411-414.
 63. Luan, C. H., Harris, R. D., Prasad, K. U. & Urry, D. W. (1990) *Biopolymers* **29**, 1699-1706.
 64. Luan, C. H., Parker, T. M., Prasad, K. U. & Urry, D. W. (1991) *Biopolymers* **31**, 465-475.
 65. Luan, C. H. & Urry, D. W. (1991) *J. Chem. Phys.* **95**, 7896-7900.
 66. Urry, D. W., Harris, R. D., Long, M. M. & Prasad, K. U. (1986) *Int. J. Peptide Protein Res.* **28**, 649-660.

Received July 31, 1992

Accepted November 11, 1992